Pergamon

Geochimica et Cosmochimica Acta, Vol. 67, No. 5, pp. 823–830, 2003

0016-7037/03 $30.00 + .00

doi:10.1016/S0016-7037(02)01276-0

Kinetics and mechanisms of the leaching of low Fe sphalerite

C. G. WEISENER, R. ST. C. SMART, and A. R. GERSON*

Ian Wark Research Institute, University of South Australia, Mawson Lakes, SA 5095, Australia

(*Received November* 26, 2001; *accepted in revised form September* 30, 2002)

Abstract—The surface speciation and leaching kinetics of 38- to 75-μm sphalerite (0.45 wt.% Fe) particles reacted in O_2 purged perchloric acid (at pH 1.0) at 25, 40, 60, and 85 °C over a leach period of 144 h were investigated. In all cases, an initial rapid leach rate is observed followed by a slower leach rate. These two leach regimes can each be adequately modeled using straight-line interpolation, and thus two activation energies (E_a) have been derived. E_a for the fast and slow Zn dissolution rates were 33 $\pm$ 4 kJ mol^{-1} and 34 $\pm$ 4 kJ mol^{-1} respectively, suggesting the same rate-determining step. *Copyright © 2003 Elsevier Science Ltd*

Particles leached at 85°C for 1, 3, 8, 18, and 144 h were examined using X-ray photoelectron spectroscopy (XPS) and time of flight secondary ion mass spectrometry (ToF-SIMS). XPS indicated a progressive increase in disulfide (S_2^{2-}) concentration over the entire leach period. Polysulfide surface species ($S_{n>2}^{2-}$), which were initially observed on 3 h of leaching, increased progressively in concentration thereafter. On 144 h of leaching, elemental sulfur, S^0, was detected by XPS on the leached samples and a diffraction pattern for crystalline elemental sulfur was observed by powder X-ray diffraction. ToF-SIMS statistical analyses revealed an increase in S_2, S_3, S_4, and S_5 fragments over the first 3 h of leaching and a progressive decrease in Zn fragment intensity over the 144-h period, confirming metal deficiency and sulfur polymerisation.

The decrease in Zn leach rate is attributed to the formation of a thick continuous metal-deficient polysulfide surface layer, which forms during the initial rapid leach stage and reaches an equilibrium thickness during the subsequent slow leach rate stage. It is proposed that either diffusion of Zn^{2+} out of, or H_3O^+ into, the polysulfide-enriched surface layer is rate-determining. The E_a are higher than expected for diffusion through a liquid (20 to 25 kJ mol^{-1}) but are commensurate with diffusion through a reacted surface layer. Continued oxidation of polysulfide surface species and the formation of elemental sulfur after prolonged leach periods do not contribute to any noticeable rate decrease and are not considered rate-determining.

1. INTRODUCTION

The dissolution of sulfide minerals in aerobic aqueous conditions is a major contributor to acid mine drainage (AMD) and toxic metal release. The effects on the environment by acid wastewater are well recognised (Alpers and Blowes, 1994; Evangelou and Zhang, 1995; Jambor and Blowes, 1994; Paktunc, 1999). It is important to the mining sector from both the environmental and economic perspectives to establish the mechanisms that govern dissolution rates of different sulfide minerals. This will enable the problem of AMD to be tackled via preventative treatments. Considerable effort has been directed toward understanding the oxidative surface reactions of the iron sulfide minerals that contribute to AMD. Conventional electrochemical methods and a variety of surface-sensitive techniques, including X-ray photoelectron spectroscopy (XPS), Auger electron spectroscopy, and scanning tunneling microscopy (STM) have been employed to elucidate these dissolution mechanisms (Buckley et al., 1989; Hochella, 1995; Karthe et al., 1993; Kim et al., 1995; Klauber et al., 2001; Laajalehto et al., 1997; Moses et al., 1987; Nesbitt and Muir, 1998).

Far fewer studies have focussed on the dissolution of zinc sulfide than pyrite (FeS_2). Vaughan and Craig (1978) reported a value for the solubility product of sphalerite of $K_{sp} = 1 \times 10^{-20.6}$ at 25°C in water. This is in agreement with Daskalakis and Helz (1993). The predominant focus has been on hydrometallurgical applications employing strong oxidising solutions of $FeCl_3$ to extract metal ions. These studies have shown a dependence of dissolution rates on ferric ion concentration, time, temperature, stirring speed, and acid concentration (Bobeck and Su, 1985; Olanipekun, 1999; Rimstidt et al., 1994). Studies by Rimstidt et al. (1994) on the reaction rates of sphalerite, galena, chalcopyrite, and arsenopyrite in ferric acid solutions demonstrated a dissolution rate for sphalerite of 7.0×10^{-8} mol m^{-2}s^{-1} and showed that sphalerite dissolved 10 times faster than chalcopyrite.

Where ferric-rich, acid-generated wastes are prevalent, surface coatings can often develop, effectively armouring sulfide minerals and thus reducing their rate of dissolution. Thomas et al. (1998) observed a reduction in dissolution rate for pyrrhotite in aerated conditions. This was attributed to the formation of metal polysulfides and iron oxy-hydroxide species. Sphalerite surfaces associated with mine wastes are often covered with iron oxides, reducing the surface area of the sphalerite exposed to solution, thus resulting in a decrease in the dissolution rate (Lin, 1997). Buckley et al. (1989) analysed the surface composition of two natural sphalerite minerals of different iron contents (1.79 wt.% Fe and 5.48 wt.% Fe) using XPS. It was shown that during leaching the dissolution of Zn resulted in a surface layer of metal-deficient sulfide and that the altered surface layer protected the sphalerite from further oxidative leaching. In hydrochloric acid solutions, the dissolution of the

* Author to whom correspondence should be addressed (Andrea.Gerson@unisa.edu.au).

Table 1. Bulk chemical analysis (wt.%) of sphalerite.

Fe	S	Zn	Cu	Pb	Si	Ca	Mn
0.45	32.52	66.28	0.08	0.28	0.30	0.07	0.01

low-iron sphalerite resulted in a less altered surface as compared to the high-Fe sphalerite.

In the study reported here, the mechanism of leaching for a low Fe sphalerite (0.45 wt.%) is examined. Low Fe sphalerite was chosen so that the dissolution rate and surface layer formation in the absence of major impurities could be established. The dissolution kinetics of Zn has been determined and the evolution of surface polymeric sulfur species measured using XPS and time of flight secondary ion mass spectrometry (ToF-SIMS). The strength of ToF-SIMS lies in its extreme surface sensitivity (1 to 2 monolayers) and detection limits (~ppb). ToF-SIMS in conjunction with XPS can provide a detailed surface layer characterisation for both the surface (ToF-SIMS) and near-surface regimes (XPS).

2. MATERIAL AND METHODS

2.1. Mineral Preparation

The 0.45 wt.% Fe -containing sphalerite (Carthage, Tennessee) used in this study was supplied by Wards Scientific Ltd (New York). Optical microscopy performed on polished sections of the Carthage sphalerite showed no evidence of other associated mineral phases (i.e., chalcopyrite, pyrite, galena, etc.). This was also confirmed by scanning electron microscopy/energy-dispersive X-ray analysis (SEM/EDX). The bulk chemical analysis of the 38 to 75 μm size fraction was carried out by acid digest followed by inductively coupled plasma atomic emission spectroscopy (Table 1). The analysis shows that the sphalerite mineral used in these experiments is 98.80% pure with the remaining ~1.20% comprised of trace impurities. Fe (0.45 wt.%) and Pb (0.28 wt.%) are the only significant impurities.

The mineral samples were dry crushed and sieved in an enclosed glove bag purged with inert gas (dry N_2) to minimise oxidation of the freshly ground sphalerite surfaces before introduction into the closed reaction vessel. A 38- to 75-μm size fraction was collected using a combination of stainless steel mesh sieves. The final sample was rinsed with methanol to minimise any attached fine particles that could bias surface area normalised rate determinations. Scanning electron micrographs before and after this treatment (Fig. 1) illustrate its effectiveness. The initial surface area of the sphalerite size fraction used in the leaching experiments was determined by the BET technique based upon krypton gas adsorption isotherms and was found to be 0.51 $\pm$ 0.05 m^2g^{-1}.

Table 2. Zn dissolution rates and E_a ($\pm$ 1 standard deviation).

Temperature (°C)	Fast rate Zn (mol $m^{-2}s^{-1}$)	E_a (kJ mol^{-1})	Slow rate Zn (mol $m^{-2}s^{-1}$)	E_a (kJ mol^{-1})	Transition (h)
25	5.75×10^{-9}	33 $\pm$ 4	1.14×10^{-9}	34 $\pm$ 4	8.6
40	1.55×10^{-8}		3.54×10^{-9}		7.2
60	1.70×10^{-8}		4.51×10^{-8}		7.0
85	6.93×10^{-8}		1.43×10^{-8}		4.4

2.2. Batch Reactor Leach Method

Leach experiments were carried our using a sealed batch reactor vessel consisting of a Teflon stirring impeller, a thermometer to monitor solution temperature, condenser to prevent solvent loss, a gas purge inlet for the introduction of O_2, and an extra port for pH measurements and sampling during experiments. A 1 dm^3 reagent grade perchloric acid solution adjusted initially to pH 1.0 was aerated with O_2 and heated in a temperature-controlled oil bath to the desired temperature (25, 40, 60, and 85 °C). Perchloric acid was chosen as its anion does not complex significantly with mineral surfaces. Also, perchloric acid does not interfere or complicate the S oxidation products that form on the mineral surface. Sulfuric and HCl acids, on the other hand, can lead to surface artifacts which can complicate both the mechanism and the XPS and TOF-SIMS spectral interpretation.

Five grams of the washed sieved sphalerite was introduced into the reaction vessel. Solution aliquots of 3 mL were collected periodically over the 144-h leach period. Solution elemental concentrations of Zn and S were analysed using inductively coupled plasma atomic emission spectroscopy. Dissolution rates for Zn were determined per unit surface area.

2.3. Sample Preparation for Surface Analysis

Samples of sphalerite for surface analyses and X-ray diffraction (XRD) measurements were prepared using the same conditions as described in Section 2.1 and leached as described in Section 2.2 at 85°C. Samples were collected after 1 h, 3 h, 8 h, 18 h, and 144 h. The sample slurry was decanted and washed with pH-adjusted perchloric acid solution, transferred to an Ar purged specimen tube, and stored in a freezer. All surface studies were performed within hours of sampling to minimise any long-term storage effects.

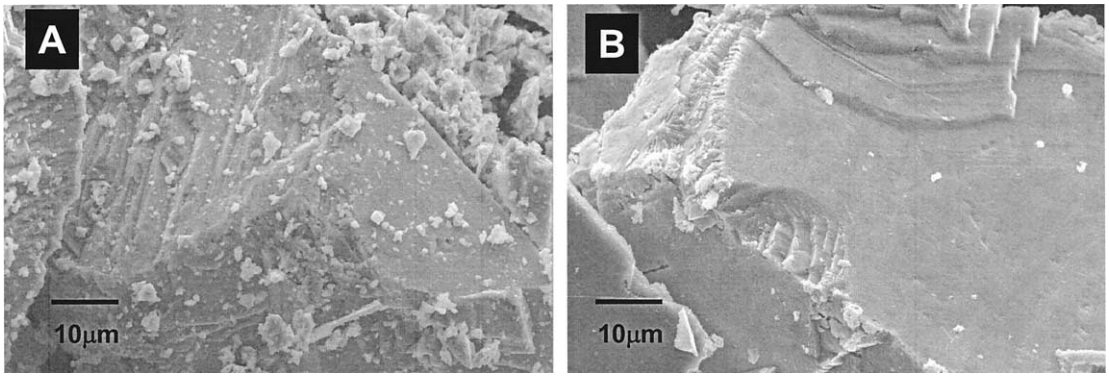

Fig. 1. (A) SEM micrograph of freshly ground sphalerite that has not been methanol washed (38 to 75 μm). (B) SEM micrograph of ground sphalerite rinsed with methanol, thus minimizing fine particle attachment.

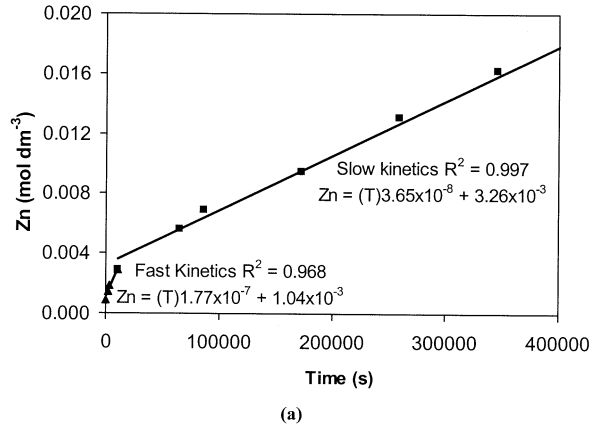

(a)

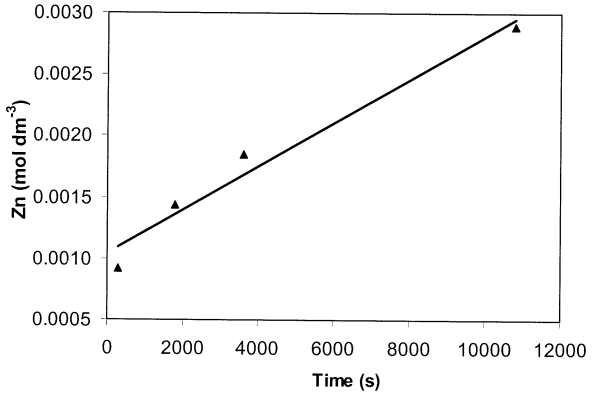

(b)

Fig. 2. The dissolution of ZnS at 85°C pH 1 shows two distinct rate regimes characterized by fast and slow leach rates (a). The last point of the fast kinetic regime is the same as the first point of the slow kinetic regime. The slow kinetic regime is also shown in (b). These graphs demonstrate that a straight line fit provides an acceptable model for both the fast and slow kinetic regimes.

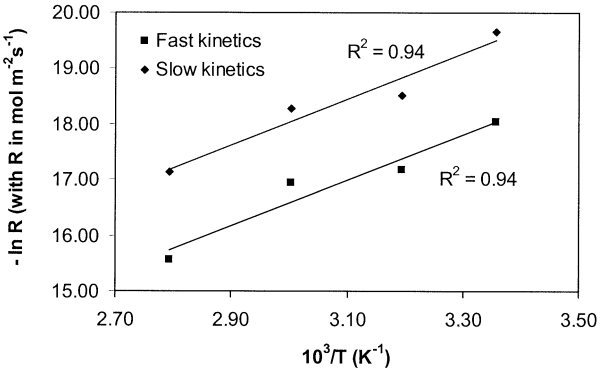

Fig. 4. Arrhenius plots for the two different kinetic regimes during the dissolution of sphalerite in perchloric acid at pH 1.

2.4. XPS

Each sample was allowed to warm to room temperature. The wet slurry was removed from the Ar-purged, sealed sample specimen container. Samples were positioned onto conductive carbon tape and arranged on an XPS specimen holder. Once positioned, the sample holder was placed into a transfer vessel. The wet sample was then introduced into the instrument. The excess moisture on the mineral surface acts as a protective barrier against further oxidation. Any residual moisture is evacuated in the introduction chamber. A cold stage was used during all XPS experiments maintaining sample temperatures at 150 K. This reduces the potential volatility of surface species, in particular elemental sulfur.

Each sample was characterised by examining the C(1s), S(2p), Fe(2p), O(1s), and Zn(2p) regions. The XPS operating pressure in the system during measurement was 2×10^{-8} torr. The expected binding energy (E_b) for the adventitious carbon C(1s) spectra (284.8 eV) was used to correct for sample charging. The low Fe-containing sphalerite, both leached and unleached, exhibited a ≈4-eV charge shift to higher E_b. This was corrected by adjusting the entire spectra so that the C(1s) E_b corresponded to 284.8 eV. S(2p) spectra were fitted and the separation and intensity ratio of the $S(2p_{1/2})$ and $S(2p_{3/2})$ components was constrained to 1.18 eV and 1:2, respectively. All S(2p) E_b refer to the

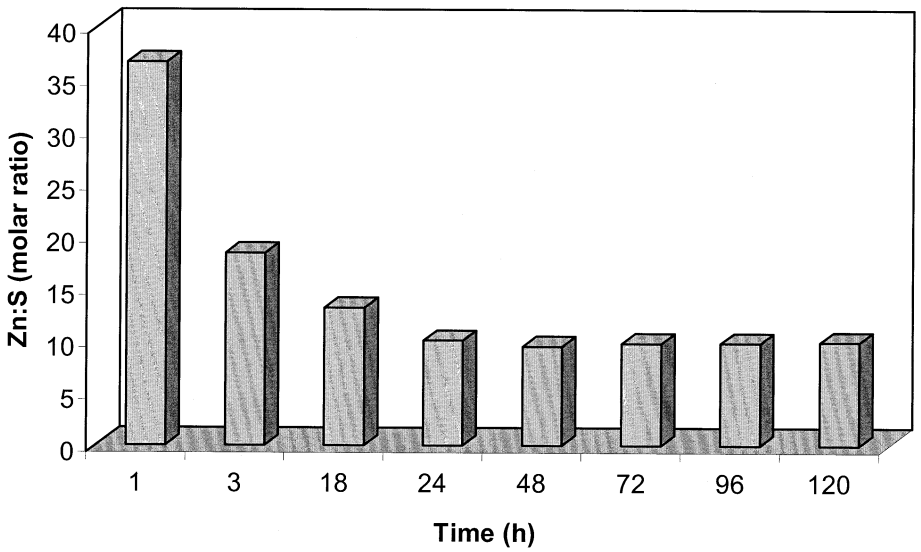

Fig. 3. Zn:S solution concentration ratios during the dissolution of ZnS at 85°C in pH 1 perchloric acid. These ratios show an initial elevated ratio after 1 h of approximately 30:1, which then drops to approximately 10:1 and remains relatively constant from 24 to 120 h of leaching.

Table 3. The leach rates and E_a for sphalerite dissolution from the literature and this study.

Reference	Fe (wt.%)	pH range	T range (°C)	Oxidant	In(R) (mol $m^{-2}s^{-1}$)	E_a (kJ mol^{-1})
Rimstidt et al. (1994)	1.0	2.0	40–60	Fe^{3+}	≈−7.67	27[b]
Bobeck and Su (1985)	6.2	2.0	47–87	Fe^{3+}	[c]	46 ± 11.3
Crundwell (1987)	0.5	1–1.5	45–85	Fe^{3+}	[c]	59[b]
	4.3				[c]	44[b]
	7.2				[c]	51[b]
	9.7				[c]	32[b]
Olanipekun (1999)	7.2	NA	70–90	Fe^{3+}	[c]	31[b]
Perez and Dutrizac (1991)	0.1	NA	50–90	Fe^{3+}	[c]	70[b]
	2.0				[c]	55[b]
[a]Fast	0.5	1	25–85	O_2	≈−7.15	34 ± 4
[a]Slow	0.5	1	25–85	O_2	≈−7.86	34 ± 3

[a] This study.
[b] No standard deviation reported.
[c] Rates in other units not comparable with this study.
NA = not available.

$S(2p_{3/2})$ component. A modified Shirley type background was used for background subtraction. All elemental concentrations derived from XPS spectra have been normalised to exclude C and O contributions.

2.5. ToF-SIMS

ToF-SIMS spectra were collected using a PHI Model 2100 TRIFT II system. A pulsed gallium beam was used at 15 kV and 60 pA to analyse a 150 × 150 μm area at high mass resolution (i.e., $\Delta m/m = 7000$ for silicon). For the high spatial resolution required in the collection of ion maps, a pulsed gallium ion beam operated at 25 kV and 600 pA was employed. No charge neutralisation was required as any charge buildup on the material surface is discharged between the pulsed sequences. The operating pressure in the system was 2×10^{-9} torr.

The same sample mounting procedure as for the XPS wet slurry samples was adopted for the samples for ToF-SIMS analysis. ToF-SIMS spectra were collected from 21 particles for each time period analysed. Both positive and negative ions were monitored. For comparative purposes, fragment intensities were normalised against the total fragment yield (i.e., the total of ^{12}C, ^{16}O, ^{17}OH, ^{23}Na, ^{27}Al, ^{32}S, ^{39}K, ^{56}Fe, ^{63}Cu, $^{64}S_2$, ^{64}Zn, $^{73}FeOH$, ^{79}CuO, $^{80}SO_3$, $^{96}S_3$, $^{128}S_4$, and $^{160}S_5$). A Student *t*-test was used to statistically analyse the data providing a 95% confidence level for all of the mean intensities. This statistical procedure has been described by Piantadosi et al. (2000).

3. RESULTS AND DISCUSSION

3.1. Zn Leach Kinetics

Two distinct rate regimes, a rapid rate followed by a slower rate, are observed during the dissolution of sphalerite at each temperature (25, 40, 60, and 85 °C, Table 2). Straight line interpolations to each rate (8 in total) had R^2 values of >0.95 (for example, Fig. 2). In all cases the last data point for the fast kinetic regime is the same as the first data point for the slow kinetic regime. The fast kinetic regime is represented by at least 4 data points for each temperature, and the slow kinetic regime is represented by at least 5 data points for each temperature. Activation energies (E_a) were calculated for both the fast and

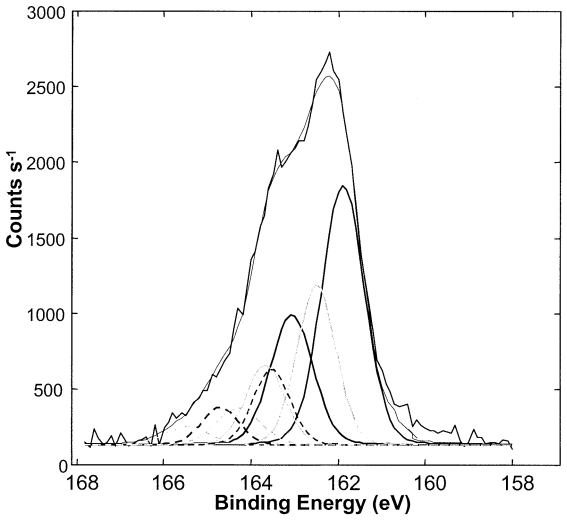

Fig. 5. Curve-fitted S(2p) spectra from a sphalerite surface subjected to 144 h of leaching. —— S^{2-}, E_b161.8 eV, —— S_2^{2-}, E_b 162.5 eV,- - - $S_{n>2}^{2-}$, E_b 163.4 eV and - - - - S^0, E_b 164.1 eV.

Table 4. XPS total S and Zn concentrations.

Leach time (h)	S(2p) (at.%)	Zn(2p) (at.%)	S:Zn molar ratio
Ground under N_2	50	50	1.0
1	56	44	1.3
3	57	43	1.3
8	61	39	1.6
18	64	36	1.8
144	74	26	2.8

Table 5. XPS S(2p) analysis of sphalerite surfaces leached over a 144-h period.

Leach time (h)	S^{2-} E_b 161.8 eV (at.%)	S_2^{2-} E_b 162.5 eV (at.%)	$S_{n>2}^{2-}$ E_b 163.4 eV (at.%)	S^0 E_b 164.1 eV (at.%)
Ground	47	3	0	0
1	49	7	0	0
3	47	7	3	0
8	40	10	11	0
18	42	10	12	0
144	40	17	14	3

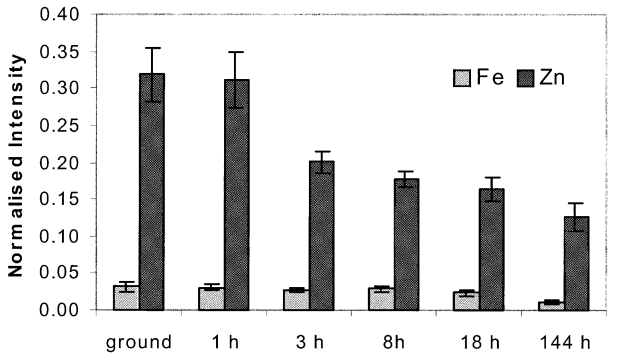

Fig. 6. A statistical analysis of positive ToF-SIMS ion data. A gradual decrease in Zn on the surface of sphalerite as a function of leach time is observed, indicating the formation of a metal-deficient surface layer.

slow leach regimes (Table 2). The time of transition from the rapid rate to the slow rate (Table 2) decreases as temperature increases.

On the introduction of the sphalerite to solution, a strong H_2S smell is noted which disappears within the first 1 to 3 h. At later stages (>100 h), elemental sulfur appears on the inside of the lid of the reaction vessel. At 85°C the Zn:S ratio in solution at 1 h of leaching is ≈30:1. This decreases progressively to ≈10:1 at 24 h of leaching (Fig. 3) and then remains relatively constant for the remaining period of the leach.

Figure 4 shows the Arrhenius plots used to calculate the E_a for the fast and slow Zn leach rate regimes. These are 34 ± 4 and 34 ± 3 kJ mol^{-1}, respectively. The E_a obtained in this study and those reported in the literature are given in Table 3. They show a wide range of values, and in many cases no standard deviation is reported.

The E_a and rates of sphalerite dissolution determined here agree with some of those obtained previously; Crundwell (1987) and Olanipekun (1999). An E_a of 34 k mol^{-1} may indicate that the rate-determining step is a chemical reaction. An E_a in the region of 20 to 25 kJ mol^{-1} would generally indicate a solution diffusion-controlled process. The higher E_a observed does not rule out the possibility of a diffusion-controlled mechanism where the diffusion is occurring through a solid, in this case a reacted surface layer, rather than through solution. The surface analytical results described below provide evidence for a diffusion-controlled dissolution mechanism and a possible explanation as to why two leach rates are observed for each leach experiment.

3.2. XPS Analysis of Leached Sphalerite Surfaces

XPS measurements were performed on a freshly ground surface of the 0.45 wt.% Fe -containing sphalerite. The measured S:Zn at.% ratio of 1.86:1 was calculated using the XPS sensitivity factors for S(2p) and Zn(2p) of 0.717 and 2.768, respectively. The stoichiometry for this mineral should be 1:1. S:Fe ratio measurements performed on freshly ground pyrite show the correct 2:1 ratio.

The S(2p) speciation of the surface was comprised of 61 at.% S^{2-} (E_b 161.8 eV) and 4 at.% S_2^{2-} (E_b 162.5 eV). If there was actually excess S in the surface layers as implied by the S:Zn ratio, the S would then have to be in the form of oxidised species, for instance polysulfides, elemental sulfur, or oxy-sulfur species, to maintain surface charge neutrality. Because the correct ratio is found for pyrite, it appears that Zn is underestimated on the surface.

Other researchers have also observed anomalous S:Zn ratios. For instance, Buckley et al. (1989) observed a 1.2:1 S:Zn ratio. The underestimation of the surface Zn concentration may be due to inaccuracy in the Zn(2p) sensitivity factor or it may be due to the different escape depths of the S(2p) and Zn(2p)

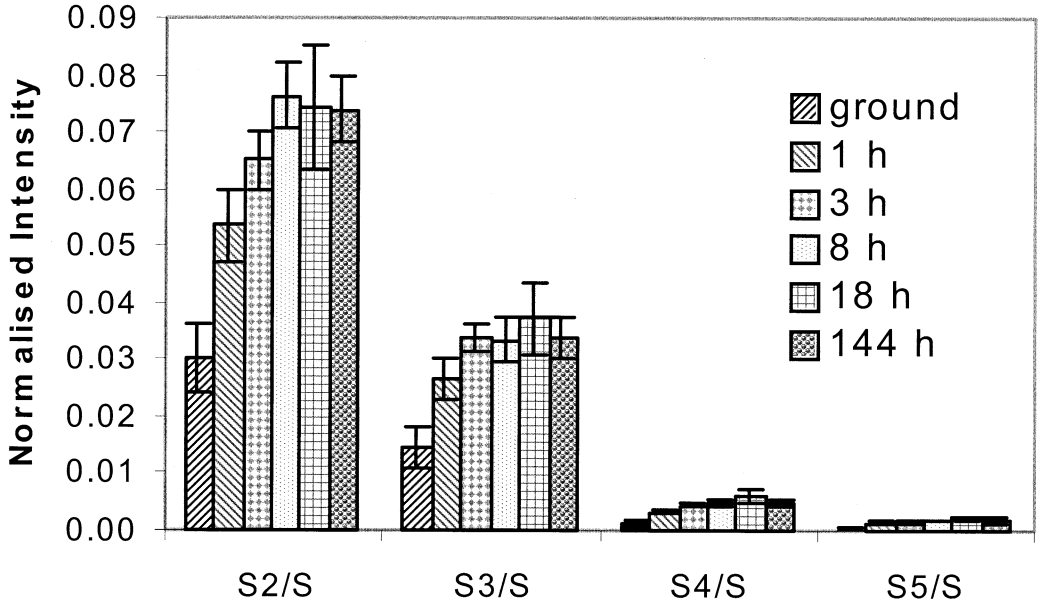

Fig. 7. A statistical analysis of negative ToF-SIMS ion data. The analysis shows increasing polymerisation of sulfur species on the sphalerite surface (1 to 2 monolayers) within the first 3 h of leaching.

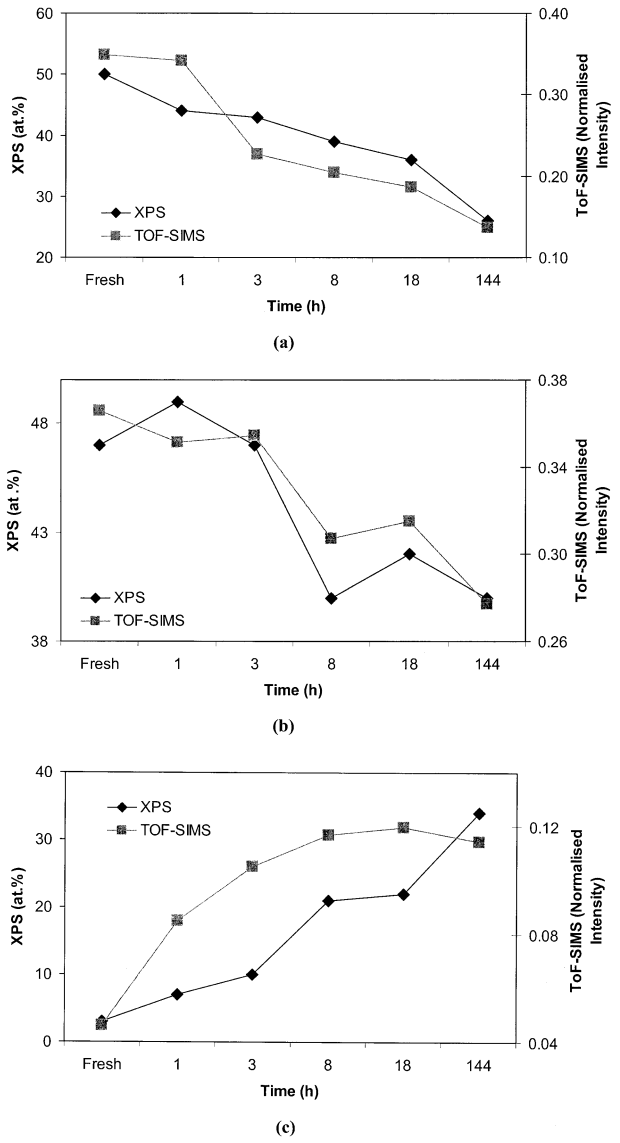

Fig. 8. Comparisons of XPS and ToF-SIMS measurements as a function of leach time, (a) metal concentration, (b) ^{32}S distribution as measured by ToF-SIMS and S^{2-} as measured by XPS, (c) total of S_n fragments as measured by ToF-SIMS and total of S_n^{2-} and S^0 as measured by XPS.

photoelectrons. The escape depths of Fe(2p) and S(2p) photoelectrons are similar, whereas the escape depth for the Zn(2p) photoelectron is significantly less than that for S(2p). Therefore, it is possible, assuming a surface layer of hydrocarbon contamination over the mineral surface, that greater attenuation of the Zn(2p) signal results as compared to the S(2p) signal. Thus, a S:Zn ratio greater than 1 may arise. However, for pyrite where the escape depths for Fe(2p) and S(2p) are more similar, the signal attenuation is also similar and the correct 2:1 S:Fe ratio results.

The S:Zn ratio observed for the fresh sphalerite surfaces does not negate the comparison of the leached surfaces as the same error is carried through the entire series and does not affect the increase in sulfur observed on the surface with progressive leaching. Moreover, no significant changes in either the C or O surface concentrations were observed and therefore there is no evidence to suggest significantly changing surface layer hydrocarbon contamination. However, to rectify the misleading S:Zn ratio we have altered the Zn(2p) sensitivity factor from 2.768 to 5.140 so that a 1:1 S:Zn ratio on the freshly ground surface results. The results shown in Tables 4 and 5 are based on this revised Zn(2p) sensitivity factor.

A series of XPS spectra were collected from the sphalerite particles leached at 85°C to determine the extent of Zn depletion and S oxidation during the dissolution (1, 3, 8, 18, and 144 h). The at.% obtained for total S and Zn given in Table 4 indicates progressive loss of Zn relative to S as leaching proceeds with a final S:Zn ratio of 2.8:1 at 144 h. A curve-fitted S(2p) spectra for the 144-h leach period is shown in Figure 5.

The changes observed in the S(2p) spectra over the 144-h leach period are not associated with the ≈4-eV charge shift and are representative of the formation of sulfur oxidation species. If broadening were occurring due to nonuniform sample charging (and not progressive S oxidation), then the same broadening of the spectra would be apparent for each leach sample. This is not the case. Although some broadening due to differential charging may have occurred, this is likely to be accommodated in the relatively broad full width half maximum (FWHM) of the polysulfide species. The leached sphalerite surfaces show a progressive increase in oxidised S species over the 144-h leach period (Table 5). The surface concentration of S_2^{2-} (E_b 162.5 eV) increases over the entire leach period. $S_{n>2}^{2-}$ (E_b 163.4 eV) is first observed on 3 h of leaching and increases in concentration over the remainder of the leach period.

The surface of the sphalerite sample leached for 144 h showed a 14 at.% increase in S_2^{2-}, a 14 at.% increase in polysulfide species (E_b 163.4 eV) relative to the freshly ground surface. In addition, 3 at.% of elemental sulfur, S^0, (E_b 164.1eV) was also present. Crystalline elemental sulfur, on the surface of the 144-h leached sample, was identified by XRD but none was detected on the samples leached for shorter periods.

It is possible that the rate-determining step for ZnS dissolution is related to the chemical potential gradient between the mineral/polysulfide interface and the polysulfide/solution interface. We propose that the change from the rapid to slow leach rate is related to the thickness of the reacted polysulfide layer and that this layer reaches a steady-state thickness at the beginning of the slow leach period. For the leach carried out at 85°C, the transition from the rapid to slow kinetic regime occurs at 4.4 h. At 8 h of leaching, as compared to 3 h the $S_{n>2}^{2-}$ content of the surface increases by 8 at.%, the S_2^{2-} content increases by only 3 at.%, whereas the S^{2-} content decreases by 7 at.%. It appears therefore that the change in rate is related to the polysulfide formation. On 144 h of leaching, 3 at.% of S^0 is observed by XPS. However, crystalline elemental sulfur is also observed by XRD, suggesting that more than 3 at.% is actually present. As the rate of Zn release remains the same on 144 h of leaching, it is apparent that elemental S does not affect the Zn leach rate.

3.3. ToF-SIMS Analysis of Leached Surfaces

The surfaces of the particles sampled at 1, 3, 8, 18, and 144 h of leaching in perchloric acid at 85°C were analysed using

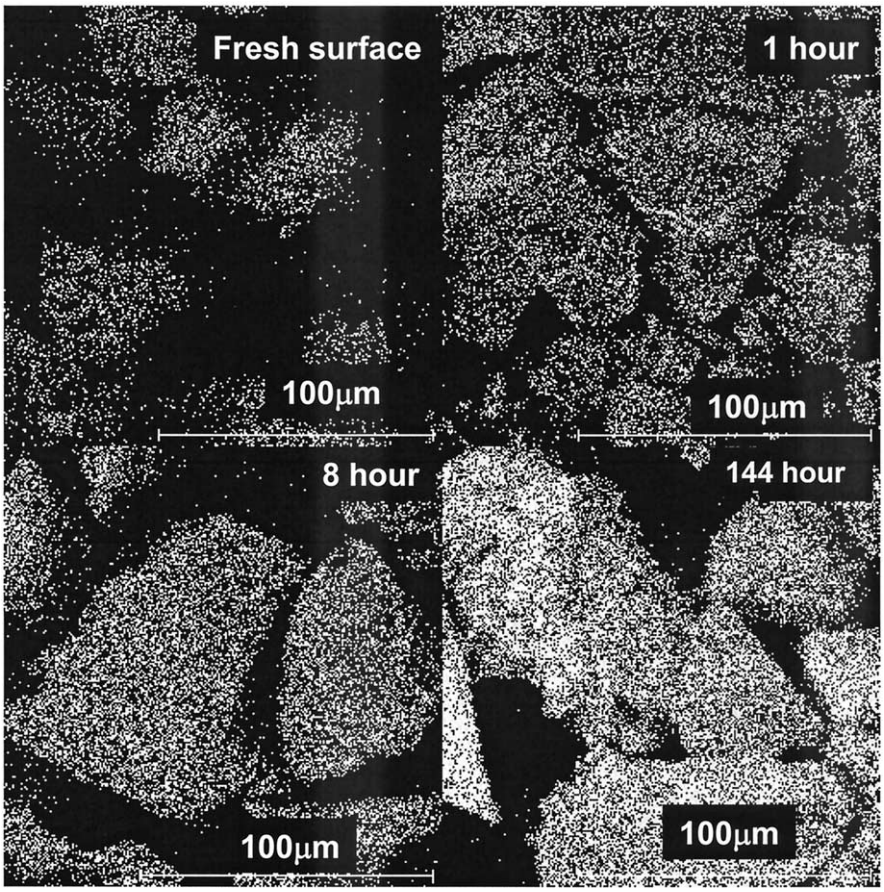

Fig. 9. ToF-SIMS images of the S_3 fragment show the surface distribution of this species as a function of leach time.

ToF-SIMS. Normalised and statistically analysed ToF-SIMS data from 21 particles were analysed to identify differences in the surface concentrations of Fe, Zn, S fragments as a function of leach time. The Fe present within the sphalerite sample was detected by ToF-SIMS.

The ToF-SIMS data (Fig. 6) indicated a decrease, over the 144-h leach period, in both Zn and Fe on the surface of the sphalerite particles. During the first 18 h the surface concentration of Zn is reduced by 50%, confirming XPS Zn(2p) analyses which showed a progressive metal loss from the surface. Only a marginal decrease in Zn is observed between 18 and 144 h of leaching, suggesting that the surface is approaching steady state with respect to Zn release from the solid.

ToF-SIMS analysis, in agreement with XPS results, indicates the presence of S_2 species on the freshly ground surface (Fig. 7). XPS analyses a depth of 3 to 5 nm. A surface concentration of 3 at.% of S_2^{2-} is derived from XPS data. The surface depth probed by ToF-SIMS (1 to 2 monolayers) would most likely be even richer in this species. It is also likely therefore that a minor concentration of longer chain polysulfides (S_3, S_4, and S_5) would also be present although these, to some extent, may be a result of the impact mechanism or recombination in vacuum.

ToF-SIMS indicates a steady increase in polymeric sulfur species (S_2/S, S_3/S, S_4/S, and S_5/S) during the first 3 h of leaching, with no further increase on additional leaching (Fig. 7). This is in qualitative agreement with XPS results, which showed a rapid increase in polysulfide species ($S_{n>2}^{2-}$) up until 8 h of leaching. This correlation strongly indicates that long-chain oligomeric species as detected by ToF-SIMS are not solely due to the impact mechanism or subsequent recombination of species in vacuum but are representative of changing surface speciation. These results imply that after 3 h the thickness of the polysulfide layer was greater than the analysis depth of ToF-SIMS. Smart et al. (2000) identified a similar correlation between XPS and ToF-SIMS data for the formation of $S_{n>2}^{2-}$ on galena and pyrrhotite. The ToF-SIMS results, in conjunction with XPS and XRD results, strongly suggested increasing S polymerisation as a function of increasing oxidation.

Figure 8 shows correlations between XPS and ToF-SIMS data. The correlation is good for the surface metal species (Fig. 8a) and the monosulfide species (Fig. 8b). In Figure 8c is shown a comparison of the trends of the evolution of S_n (the total fragments containing from 2–5 S) as measured by ToF-SIMS and S_n^{2-} (bisulfides and polysulfides) plus S^0 as measured by XPS. These data indicate that the concentration of surface polysulfide fragments ($n \geq 2$) increases more rapidly in the surface region (1 to 2 monolayers as measured by ToF-SIMS) than in the near-surface region (3 to 5 nm, as measured by XPS).

Secondary ion images (Fig. 9) show the relatively uniform distribution of S_3 polymer species and the increase in these species on leaching. There are no localised areas of higher concentrations that might be associated with elemental sulfur. This may be due to the loss of elemental S in vacuum.

4. CONCLUSIONS

The decrease in Zn dissolution rate is attributed to the formation of metal-deficient polysulfide surface layers, which form during an initially rapid leaching period. The rate of dissolution of sphalerite is determined by the chemical potential gradient between the reacting sphalerite/polysulfide interface and the polysulfide/solution interface. The thickness of the polysulfide layer increases during the initial rapid leach period and reaches steady state during the slow leach period. It is proposed that the rate-controlling step is either Zn^{2+} diffusion through the S-enriched surface layer or diffusion of H_3O^+ from the solution interface to the unreacted ZnS. Continued oxidation of S species gives rise to polysulfides and finally elemental sulfur surface species over prolonged leach times. The elemental sulfur does not contribute to any noticeable decrease in the kinetics once it forms and is not considered rate-determining.

Associate editor: G. Sposito

REFERENCES

Alpers C. N. and Blowes D. W. (1994) *Environmental Geochemistry of Sulfide Oxidation*. American Chemical Society, Washington, DC.

Bobeck G. E. and Su H. (1985) The kinetics of dissolution of sphalerite in ferric chloride solution. *Metallurgical Transactions B* **16b,** 413–424.

Buckley A. N., Wouterlood H. J., and Woods R. (1989) The surface composition of natural sphalerites under oxidative leaching conditions. *Hydrometallurgy* **22,** 39–56.

Crundwell F. K. (1987) Kinetics and mechanism of the oxidative dissolution of a zinc sulphide concentrate in ferric sulphate solutions. *Hydrometallurgy* **19,** 227–242.

Daskalakis K. D. and Helz G. R. (1993) The solubility of sphalerite (ZnS) in sulfidic solutions at 25 C and 1 atm pressure. *Geochim. Cosmochim. Acta* **57,** 4923–4931.

Evangelou V. P. and Zhang Y. L. (1995) A review: Pyrite oxidation mechanisms and acid mine drainage prevention. *Crit. Rev. Environ. Sci. Technol.* **25**(2), 141–199.

Hochella M. F. J. (1995) Mineral surfaces: Their characterization and their chemical, physical and reactive nature. In *Mineral Surfaces* (eds. D. J. Vaughan and R. A. D. Pattrick), pp. 17–86. Chapman & Hall, London.

Jambor J. L. and Blowes D. W. (1994) *Short Course Handbook on Environmental Geochemistry of Sulfide Mine-Wastes*. Mineralogical Association of Canada, Nepean.

Karthe S., Szargan R., and Suoninen E. (1993) Oxidation of pyrite surfaces: A photoelectron spectroscopic study. *Appl. Surface Sci.* **72,** 157–170.

Kim B. S., Hayes R. A., Prestidge C. A., Ralston J., and Smart R. St. C. (1995) Scanning tunneling microscopy studies of galena: The mechanisms of oxidation in aqueous solution. *Langmuir* **11,** 2554–2562.

Klauber C., Parker A., van Bronswijk W., and Watling H. (2001) Sulphur speciation of leached chalcopyrite surfaces as determined by x-ray photoelectron spectroscopy. *Int. J. Miner. Process.* **62,** 65–94.

Laajalehto K., Kartio I., and Suoninen E. (1997) XPS and SR-XPS techniques applied to sulphide mineral surfaces. *Int. J. Miner. Process.* **51**(1–4), 163–170.

Lin Z. (1997) Mineralogical and chemical characterisation of wastes from the sulfuric acid industry in Falun, Sweden. *Environ. Geol.* **30,** 153–161.

Moses C. O., Nordstrom D. K., Herman J. S., and Mills A. L. (1987) Aqueous pyrite oxidation by dissolved oxygen and by ferric iron. *Geochim. Cosmochim. Acta* **51,** 1561–1571.

Nesbitt H. W. and Muir I. J. (1998) Oxidation states and speciation of secondary products on pyrite and arsenopyrite reacted with mine waste waters and air. *Mineral. Petrol.* **62,** 123–144.

Olanipekun E. O. (1999) Kinetics of sphalerite leaching in acidic ferric chloride solutions. *Trans. Indian Inst. Metallurgy* **52**(2–3), 81–86.

Paktunc A. D. (1999) Characterization of mine wastes for prediction of acid mine drainage. In *Environmental Impacts of Mining Activities—Emphasis on Mitigation and Remedial Measures* (ed. J. M. Azcue), pp. 19–40. Springer, Ottawa.

Perez I. P. and Dutrizac J. E. (1991) The effect of iron content of sphalerite on its rate of dissolution in ferric sulphate and ferric chloride media. *Hydrometallurgy* **26,** 211–232.

Piantadosi C., Jasieniak M., Skinner W. M., and Smart R. St. C. (2000) Statistical comparison of surface species in flotation concentrates and tails from ToF-SIMS evidence. *Mineral Engin.* **13**(13), 1377–1394.

Rimstidt J. D., Chermak J. A., and Gagen P. M. (1994) Rates of reaction of galena, sphalerite, chalcopyrite, and arsenopyrite with Fe(III) in acidic solutions. In *Environmental Geochemistry of Sulfide Oxidation*, Vol. 550 (eds. C. N. Alpers and D. W. Blowes). American Chemical Society, Washington, DC.

Smart R. St. C., Jasieniak M., Prince K. E., and Skinner W. M. (2000) SIMS studies of oxidation mechanisms and polysulfide formation in reacted sulfide surfaces. *Mineral Engin.* **13**(8–9), 857–870.

Thomas J. E., Jones C. F., Skinner W. M., and Smart R. St. C. (1998) The role of surface sulfur species in the inhibition of pyrrhotite dissolution in acid conditions. *Geochim. Cosmochim. Acta* **62**(9), 1555–1565.

Vaughan D. J. and Craig J. R. (1978) *Mineral Chemistry of Metal Sulfides*. Cambridge University Press, Cambridge.